Articles

Mechanism of Neomycin and Rev Peptide Binding to the Rev Responsive Element of HIV-1 As Determined by Fluorescence and NMR Spectroscopy†

Karen A. Lacourciere, James T. Stivers, and John P. Marino*

Center for Advanced Research in Biotechnology, University of Maryland and National Institute for Standards and Technology, 9600 Gudelsky Drive, Rockville, Maryland 20850

Received December 22, 1999; Revised Manuscript Received February 17, 2000

ABSTRACT: Rev is an essential HIV-1 regulatory protein that binds the Rev responsive element (RRE) within the *env* gene of the HIV-1 RNA genome and is involved in transport of unspliced or partially spliced viral mRNA from the cell nucleus to the cytoplasm. Previous studies have shown that a short α-helical peptide derived from Rev (Rev 34−50), and a truncated form of the RRE sequence provide a useful in vitro system to study this interaction while still preserving the essential aspects of the native complex. We have selectively incorporated the fluorescent probe 2-aminopurine 2′-*O*-methylriboside (2-AP) into the RRE sequence in nonperturbing positions (A68 and U72) such that the binding of both Rev peptide and aminoglycoside ligands could be characterized directly by fluorescence methods. Rev peptide binding to the RRE-72AP variant resulted in a 2-fold fluorescence increase that provided a useful signal to monitor this binding interaction ($K_D = 20 \pm 7$ nM). Using stopped-flow kinetic measurements, we have shown that specific Rev peptide binding occurs by a two-step process involving diffusion-controlled encounter, followed by isomerization of the RNA. Using the RRE-68AP and -72AP constructs, three classes of binding sites for the aminoglycoside neomycin were unambiguously detected. The first site is noninhibitory to Rev binding ($K_D = 0.24 \pm 0.040$ μM), the second site inhibited Rev binding in a competitive fashion ($K_D = 1.8 \pm 0.8$ μM), and the third much weaker site (or sites) is attributed to nonspecific binding ($K_D \geq 40$ μM). Complementary NMR measurements have shown that neomycin forms both a specific binary complex with RRE and a specific ternary complex with RRE and Rev. NMR data further suggest that neomycin occupies a similar high-affinity binding site in both the binary and ternary complexes, and that this site is located in the lower stem region of RRE.

Rev is an important HIV-1[1] regulatory protein that binds to part of the *env* gene within the HIV-1 RNA genome, the so-called Rev responsive element (*1*−*5*). Rev is involved in the transport of unspliced and incompletely spliced viral mRNAs, which encode the structural proteins essential for viral replication, from the nucleus to the cytoplasm of the host cell. Stem−loop IIB of RRE, which contains a purine-rich internal bulge, has been identified as the high-affinity Rev binding site (*6*, *7*), and small peptides containing a 17 amino acid arginine-rich region of Rev (amino acids 34−51) have been shown to bind this stem−loop specifically (*8*−*14*). Since Rev protein binding to viral mRNA at the RRE is essential for HIV replication, acting as a crucial switch between viral latency and active viral replication, the development of new drug therapies against HIV-1 infection based on inhibitors of this essential interaction is desirable.

Members of the aminoglycoside family of antibiotics have been shown to interact with a variety of RNA molecules, including the RRE IIB stem−loop (*15*−*19*). In previous studies, it has been demonstrated that certain aminoglycosides compete with Rev peptides for binding to stem−loop IIB of RRE in vitro, as well as interfere with Rev function in vivo and thereby inhibit production of the HIV-1 virus (*15*). One such aminoglycoside, neomycin, inhibited Rev binding to RRE at a concentration ∼10-fold lower than other aminoglycosides tested. Although neomycin and other cationic aminoglycosides are not viable drug candidates, understanding the binding modes of these molecules to RRE, as well as the mechanism for inhibition of Rev binding, could provide the basis for a more targeted approach for developing drugs based on aminoglycoside scaffolds (*20*−*26*). Previously, direct binding measurements have reported K_D values in the range 80−200 nM for the interaction of neomycin with RRE in solution (*17*), while competition binding studies have

† This work was supported by an intramural award to J.P.M. and J.T.S. from the Advanced Technology Program (ATP) of the National Institute of Standards and Technology.

* Address correspondence to this author. Tel: 301-738-6160, FAX: 301-738-6255, Email: marino@carb.nist.gov.

[1] Abbreviations: RNA, ribonucleic acid; RRE, truncated version of the Rev responsive element corresponding to stem−loop IIB of the full-length 234-nucleotide sequence; HIV, human immune deficiency virus; TAR, trans-activating region of the HIV-1 genome; HPLC, high-performance liquid chromatography; Tris-HCl, tris(hydroxymethyl)-aminomethane hydrochloride; SDS, sodium dodecyl sulfate; EDTA, (ethylenedinitrilo)tetraacetic acid, disodium salt; DEPC, diethyl pyrocarbonate; 2-AP, 2-aminopurine 2′-*O*-methylriboside; MALDI, matrix-assisted laser desorption−ionization mass spectrometry; Fl-Rev, amino-terminal fluorescein-labeled Rev peptide; SPR, surface plasmon resonance; NMR, nuclear magnetic resonance; NOESY, nuclear Overhauser effect spectroscopy.

10.1021/bi992932p CCC: $19.00
Published on Web 04/14/2000

indicated that neomycin is much more weakly inhibitory toward Rev binding, with a K_i in the low micromolar range (*15, 18, 19*). It is not clear what the basis is for the large differences between the equilibrium and inhibition constants, but the possibility that the direct binding and competition methods are measuring two different binding sites for neomycin is suggested. This possibility is further suggested by neomycin binding measurements performed by surface plasmon resonance methods, which indicated a stoichiometry of 3 neomycin molecules per RRE (*16*).

Here we report a new assay based upon 2-aminopurine fluorescence that has allowed the detailed characterization of the binding of both Rev peptide and aminoglycosides to RRE stem−loop IIB. Previous studies have shown that 2-AP can be used as a valuable probe of the structure and dynamics of specific sites in DNA (*27*−*29*), as a monitor for enzyme−DNA interactions (*28, 30*−*32*), and to study Mg^{2+}-dependent conformational changes in the hammerhead ribozyme (*33*). The fluorescence of 2-AP is usually highly quenched when it is stacked with other bases, but increases as much as 100-fold when fully exposed to solvent (*34*). Thus, the quantum yield of 2-AP is highly sensitive to changes in its microenvironment, which allows the detection of subtle conformational changes in the nucleic acid upon interaction with ligands. In addition, 2-AP is a generally nonperturbing substitution since it is similar in structure to adenine (6-aminopurine) and will form a thermodynamically equivalent wobble base pair with uridine (*34*). The availability of a high-resolution structure of the RRE−Rev peptide complex (*12*), as well as detailed mutagenesis studies (*35, 36*), guided the positioning of the 2-AP probe at sites that were likely to respond to ligand binding, without altering the native interaction with Rev. The NMR structure of the Rev peptide−RRE complex indicates that two bases, A68 and U72, are flipped-out from the RNA helix upon Rev peptide binding (*12*) (Figure 1). Since the substitution of 2-AP for adenine at position 68 is conservative, and mutagenesis studies indicated that substitutions could be made at positions 68 and 72 without affecting Rev binding (*35, 36*), these two sites seemed good candidates for positioning a 2-AP probe to monitor both peptide and neomycin binding.

The results described here show that the substitution of 2-AP at position 68 or 72 afforded RRE constructs that retained the ability to bind Rev, while acting as informative reporter groups for Rev and neomycin binding. This novel fluorescence approach has revealed that Rev binding is a two-step process involving structural isomerization of the RNA, and that neomycin binds to both tight and weaker sites on RRE, where one of the weaker sites is inhibitory to Rev binding. On the basis of these findings and complementary NMR measurements, we propose a detailed structural, thermodynamic, and kinetic description of the interactions of Rev and neomycin with RRE.

EXPERIMENTAL PROCEDURES[2]

Materials. Neomycin B was purchased from Sigma (St. Louis, MO) and used without further purification. Neomycin phosphotransferase II was obtained from Eppendorf-5 Prime Inc. (Boulder, CO). All other buffers and reagents were of the highest quality commercially available and were used without further purification.

RNA and Peptide Synthesis. The 34mer RRE RNA hairpin (Figure 1A) containing the high-affinity Rev binding site was prepared by in vitro T7 polymerase runoff transcription using a synthetic DNA oligonucleotide template using the method of Milligan and Uhlenbeck (*37, 38*). DNA templates were purchased from Integrated DNA Technologies (Coralville, IA) and purified using preparative-scale denaturing polyacrylamide gel electrophoresis. 2-Aminopurine 2′-*O*-methylriboside-containing RNA oligonucleotides were synthesized on an Applied Biosystems 390 synthesizer (Perkin-Elmer, Forest City, CA) using standard phosphoramidite chemistry (*39*). The nucleoside phophoramidites were purchased from Glen Research (Sterling, VA). All RNA oligonucleotides were purified using preparative-scale denaturing polyacrylamide gel electrophoresis and recovered by electrophoretic elution. RNA samples were desalted by extensive dialysis against DEPC-treated ddH_2O using a microdialysis system. RNA concentrations were determined by measuring the absorbance at 260 nm using an extinction coefficient of 322.9 mM^{-1} cm^{-1}.

The 22 amino acid (Suc-TRQARRNRRRRWRERQRA-AAAK) arginine-rich peptide used in this study was derived from the Rev protein and previously shown to interact with high affinity to RRE stem−loop IIB (*9, 11*−*14*). The peptide was synthesized by Bio Synthesis, Inc. (Lewisville, TX), and purified using C-18 reversed-phase HPLC to a final purity of greater than 95%. MALDI-TOF (Perseptive Biosystems, Framington, MA) analysis gave a MW [MH^+] = 2950.2, which agrees well with the theoretical mass of 2950.3. Circular dichroism spectra of the peptide obtained on a Jasco J-720 spectropolarimeter (Japan, Spectroscopic, Tokyo, Japan) at 4 °C in a buffer containing 100 mM NaF and 10 mM sodium phosphate (pH 6.5) showed 28% α-helical content, which is consistent with previous reports (*9, 10*). The Rev concentration was determined from its extinction coefficient at 280 nm (5.6 mM^{-1} cm^{-1}). Amino-terminal fluorescein-labeled Rev was purchased from QCB Inc. (Hopkinton, MA), and its concentration was determined spectroscopically at 492 nm using an extinction coefficient of 78 mM^{-1} cm^{-1}.

Steady-State Fluorescence Measurements of Rev Peptide and Aminoglycoside Binding to RRE Constructs. The fluorescence of RNA oligonucleotide samples (150 μL) selectively labeled with 2-aminopurine was measured at 10 °C on a SPEX Fluoromax-2 spectrofluorometer (Instruments SA, Edison, NJ) using a 0.3 cm square cuvette. Emission spectra were recorded over the wavelength range of 330−450 nm with an excitation wavelength of 310 nm. The spectral bandpass was 5 nm for all spectra. The dissociation constant for Rev binding to RRE-72AP was determined by following the increase in fluorescence at 370 nm as a fixed concentration of the fluorescent RNA was titrated with increasing amounts of Rev. Similarly, the binding of aminoglycosides was followed by monitoring the change in 2-AP fluorescence as a fixed concentration of RRE-72AP or RRE-68AP was titrated with increasing amounts of the aminoglycoside.

[2] Certain commercial equipment, instruments, and materials are identified in this paper in order to specify the experimental procedure. Such identification does not imply recommendation or endorsement by the National Institute of Standards and Technology, nor does it imply that the material or equipment identified is necessarily the best available for the purpose.

Single-site binding of Rev or aminoglycoside was fitted to eq 1:

$$F = -\{(F_o - F_f)/2[\mathrm{RRE}]_{tot}\} \times \left\{b - \sqrt{(b^2 - 4[\mathrm{L}]_{tot}[\mathrm{RRE}]_{tot})}\right\} + F_o \quad (1)$$

$$b = K_d + [\mathrm{L}]_{tot} + [\mathrm{RRE}]_{tot}$$

where F_o and F_f are the initial and final fluorescence intensities, respectively, $[\mathrm{RRE}]_{tot}$ is the total RRE concentration, and $[\mathrm{L}]_{tot}$ is the total concentration of Rev or aminoglycoside. Aminoglycoside binding to multiple sites on RRE was modeled using the computer program *Dynafit* (*40*). Competitive displacement assays were performed to determine which aminoglycoside binding sites were inhibitory to Rev binding. For these experiments, a solution of 2-AP-labeled RRE was incubated with a fixed concentration of neomycin (or Rev peptide), and the fluorescence change was followed as increasing amounts of competing Rev peptide (or neomycin) were added to the solution. The fluorescence emission intensities at 370 nm as a function of total added ligand concentration were fitted to a given molecular mechanism by nonlinear least-squares regression using the computer program *DynaFit* (*40*). This program determines the composition of complex mixtures at equilibrium by simultaneously solving the nonlinear equations for mass balance of the component species. Thus, the observed fluorescence changes may be easily fit to a variety of user-defined models to allow the determination of the best-fit model for a given system. The details of the individual displacement experiments are described in the figure legends and under Results.

Binding Measurements Using Equilibrium Ultrafiltration. The ultrafiltration procedure previously described by Werstuck et al. (*17*) was used to confirm the fluorescence measurements for neomycin binding to RRE. Briefly, binding reactions (250 μL) containing 200 nM RRE-68AP and 0−1 μM neomycin were incubated at 10 °C for 15 min in standard buffer. Free and RRE-bound neomycin were separated by spinning the solution for 30 s in a Microcon 3 filter (Amicon, Beverly, MA). Five microliters of the flow-through and retentate was ^{32}P-labeled for 15 min at 37 °C using [γ-^{32}P]-ATP (0.5 μM) in the presence of neomycin phosphotransferase II. The reactions were terminated by incubation at 90 °C for 5 min, and 5 μL of the aqueous phase was spotted onto Whatman P81 paper. The papers were washed with 90 °C water for 5 min, and then 3 times with water at room temperature. The radioactivity was quantified by phosphorimaging using a Storm 840 (Molecular Dynamics, Sunnyvale, CA). A linear calibration plot of counts against total neomycin concentration was used to convert counts to free and bound neomycin concentration. The binding constant and stoichiometry were then determined using eq 2, where $[\mathrm{Neo}]_b$ and $[\mathrm{Neo}]_f$ are the concentrations of free and bound neomycin:

$$[\mathrm{Neo}]_b = [\mathrm{Neo}]_f[\mathrm{RRE}]_{tot}/([\mathrm{Neo}]_f + K_D) \quad (2)$$

The displacement of Fl-Rev from RRE-68AP by neomycin was followed by a similar ultrafiltration experiment. Nine binding reactions (500 μL) containing 500 nM RRE-68AP, 450 nM Fl-Rev, and 0−200 μM neomycin were incubated at 10 °C for 15 min in standard buffer. Free and RRE-bound Fl-Rev were separated by spinning the solution for 6 min at 12000*g* using a Microcon-10 filter (Amicon, Beverly, MA) such that about 170 μL of the solution passed through the membrane. One hundred and fifty microliters of the filtrate was removed, and the fluorescence at 525 nm due to free Fl-Rev was measured using 490 nm excitation, and excitation and emission slit widths of 0.5 and 4 nm, respectively. Since the fluorescence of free Fl-Rev is quenched ~35% as the neomycin concentration is increased from 0 to 200 μM, a standard neomycin quench curve was generated to allow correction for this effect. The corrected fluorescence measurements were then plotted against the total neomycin concentration, and were fitted using the program *Dynafit* (*40*) to a two-site model in which neomycin binds to one site, and then competes with Fl-Rev for binding to a second site on RRE.

Stopped-Flow Fluorescence Measurements. Stopped-flow fluorescence experiments were performed at 10 °C in the standard buffer solution containing 140 mM NaCl, 5 mM KCl, 1 mM $MgCl_2$, 1 mM $CaCl_2$, and 20 mM HEPES (pH 7.4) using a Stop-Flow device from Applied Photophysics (Surray, U.K.) in the two-syringe mode (dead time = 1.1 ms). The kinetics of Rev peptide association with the RRE-72AP construct were followed using pseudo-first-order conditions, where the peptide was present at a concentration at least 5-fold greater than the RNA. The time course of the increase in 2-AP fluorescence (F_t) as a result of peptide binding showed two kinetic phases and was fit to the double exponential expression: $F_t = F_1 \exp(-k_1 t) + F_2 \exp(-k_2 t) + C$, where F_1, F_2 and k_1, k_2 are the amplitudes and rate constants for the first and second kinetic phases, respectively, and C is a constant offset. The kinetics of dissociation of the Rev peptide from the RNA were studied using irreversible conditions by following the decrease in 2-AP fluorescence as the Rev peptide dissociates. The reaction was made irreversible by trapping the free RNA with excess neomycin, thereby preventing rebinding of the dissociated peptide. The time course was fit to a single-exponential decay: $F_t = F_1 \exp(-k_1 t) + C$, where k_1 is the observed off-rate of the peptide. In these experiments, 2-AP-containing RNA was excited at 310 nm, and the fluorescence was monitored using a 360 nm cut-on filter. Specifics of the individual experiments are described in the figure legends and text.

The concentration dependence of the observed rates of binding was fit to eq 3, which describes the two-step binding mechanism of eq 4.

$$k_{obsd} = \frac{k_1[\mathrm{Rev}](k_{-2} + k_2) + k_{-1}k_{-2}}{k_1[\mathrm{Rev}] + k_{-1} + k_{-2} + k_{-2}} \quad (3)$$

$$\mathrm{Rev} + \mathrm{RRE} \underset{k_{-1}}{\overset{k_1}{\rightleftharpoons}} \mathrm{Rev{\cdot}RRE} \underset{k_{-2}}{\overset{k_2}{\rightleftharpoons}} \mathrm{Rev{\cdot}RRE^*} \quad (4)$$

The curve-fitting program *GraFit* 4.0 (Erithacus Software) was used to obtain the observed on-rate [$k_{on} = k_1 k_{max}/(k_{-1} + k_{max})$] and to estimate the observed off-rate [$k_{off} = k_{-1}k_{-2}/(k_{max} + k_{-1})$] and the maximal rate ($k_{max} = k_2 + k_{-2}$). In addition, to ensure that a realistic model of the kinetic data was arrived at by the analytical solution to eq 2, the amplitudes and rates of the raw kinetic traces, and the concentration dependence of the kinetic data, were simulated

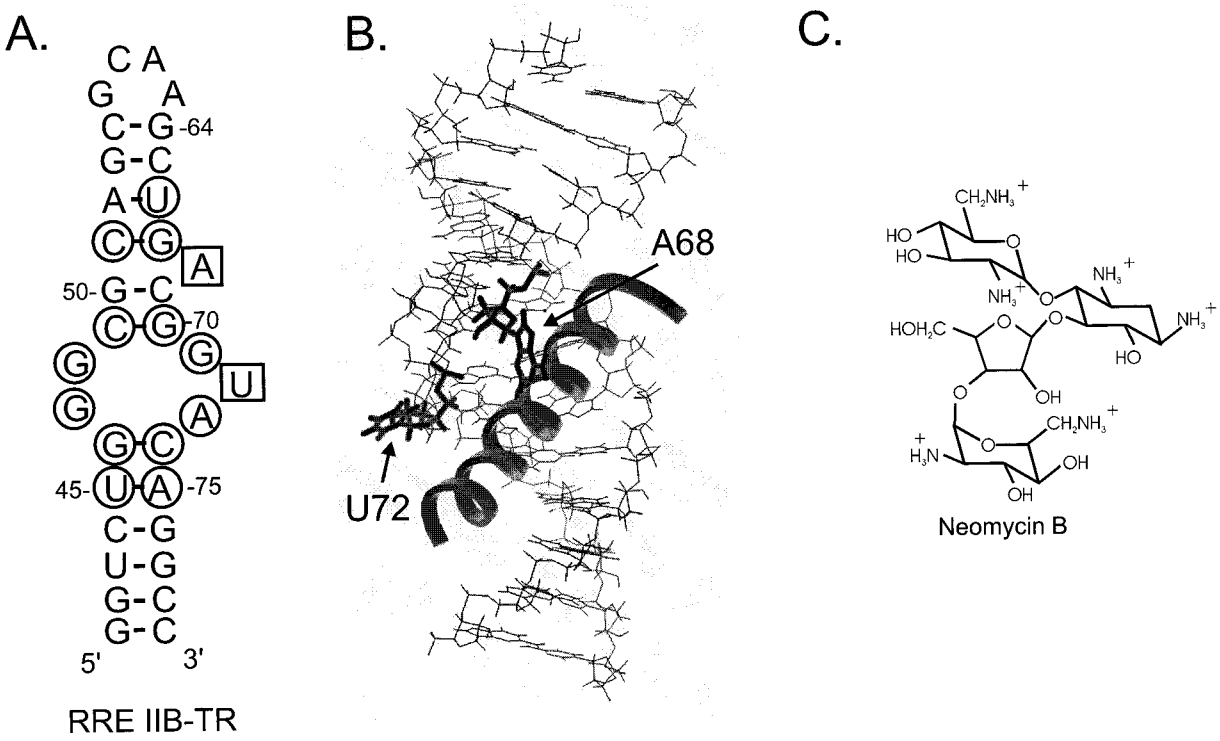

FIGURE 1: RRE RNA sequences and structure of the RRE−Rev complex. (A) Sequence of the truncated 34mer RNA hairpin derived from the RRE IIB hairpin that is used in the fluorescence and NMR studies described here. Nucleotides identified as important for Rev binding by chemical modification interference and in vitro selection data are circled. Nucleotide positions A68 and U72, which were substituted with the fluorescent probe 2-aminopurine-2′-*O*-methyl riboside (2-AP), are boxed. (B) NMR-derived structure of the RRE−Rev peptide interaction (*12*). RRE is shown in stick representation and the Rev peptide as a ribbon trace. Residues A68 and U72, which were substituted with 2-AP, are bolded. (C) Structure of the aminoglycoside neomycin B.

by numerical integration using the programs Kinsim and Fitsim (*41*). The reported uncertainties in the microscopic kinetic constants are estimated maximum errors obtained from trial and error simulations of the individual kinetic traces, and the best-fit values from curve fitting to eq 3.

NMR Spectroscopy. NMR samples were prepared to contain between 0.5 and 1.0 mM RRE in NMR buffer [25 mM NaCl, 1 mM cacodylate (pH 6.5), and 90% H_2O/10% D_2O]. A 1:1 complex of RRE with Rev peptide was formed by adding equal molar amounts of peptide from a concentrated stock (3.15 mM) to a prepared RRE NMR sample. Shigemi (Shigemi, Inc., Allison, PA) limited-volume NMR tubes were used with a final total volume of ∼250 μL for each sample. The neomycin−RRE complex was formed by titration of a concentrated stock of neomycin (10 mM) with a prepared RNA sample. The ternary neomycin−RRE−Rev complex was formed in two ways: either by titration of a concentrated stock of neomycin to the prepared RRE−Rev NMR sample or by titration of a concentrated stock of peptide to the prepared neomycin−RRE NMR sample. The formation of both the binary and the ternary complex was monitored by observation of one-dimensional imino proton NMR spectra at 15 °C.

All NMR spectra were recorded on either a Bruker AVANCE 600 MHz or a Bruker AVANCE 500 MHz spectrometer (Bruker Instruments, Billerica, MA), each equipped with a triple-resonance ^{1}H, ^{13}C, ^{15}N triple-axis gradient probe and processed using a Silicon Graphics O2 workstation. One-dimensional proton spectra were collected at 15 °C using a water flip-back Watergate pulse sequence (*42*, *43*) with a sweep width of 12 000 Hz, 4K complex points, and 256 scans and processed using 5 Hz line-broadening in XWINNMR 2.6 software (Bruker Instruments). Two-dimensional NOESY spectra were recorded at 15 °C, using water flip-back Watergate water suppression (*43*). NOESY spectra were collected with a mixing time of 150 ms and sweep widths of 12 000 Hz in both dimensions, 4K by 256 complex data points in t_2 and t_1, respectively, and 64 scans per increment. Two-dimensional data were processed using NMRPipe (*44*) software. 2D NOESY spectra were apodized using 60° and 90° shifted sine bell functions over 512 and 256 complex points in the t_2 and t_1 dimensions, respectively, and zero-filled to 2048 real points in both dimensions.

Error Analysis. The reported errors are the standard uncertainties of the data from the best-fit theoretical curves. This method assumes that the standard uncertainty of the measurement is approximated by the standard deviation of the points from the fitted curve (*45*).

RESULTS

Binding of Rev Peptide to 2-AP-Labeled RRE. The binding of Rev peptide and neomycin B to RRE was directly monitored by incorporating the fluorescent nucleotide probe 2-aminopurine 2′-*O*-methylriboside (2-AP) in positions 68 and 72 of the RNA sequence (Figure 1A,B). In Figure 2A,B, it is shown that the intensity of the 2-AP emission spectrum of RRE-72AP increases in a saturable fashion as the concentration of Rev peptide is increased, with a maximal increase of about 2-fold. The direction of this fluorescence change indicates that the 72AP base becomes on average less stacked upon Rev peptide binding, which is consistent with the exposed position of U72 in the NMR structure of

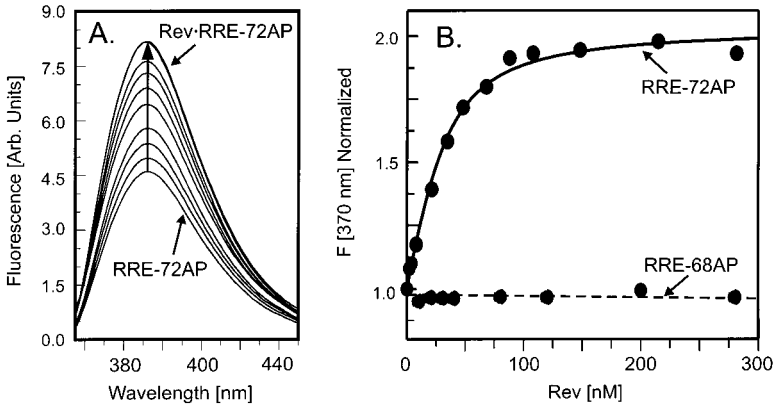

FIGURE 2: Fluorescence changes accompanying titration of 2-AP-labeled RRE with Rev peptide. (A) Titration of 100 nM RRE-72AP with increasing concentrations of Rev peptide. (B) Plot of the relative fluorescence increase at 370 nm as a function of total Rev concentration. The solid curve is a fit to eq 1 ($K_D = 13 \pm 2$ nM). A similar titration of the RRE-68AP with Rev produced no significant change in fluorescence (dashed line).

Table 1: Thermodynamic and Kinetic Parameters for Rev and Neomycin Binding to RRE RNA[a]

components	K_D (μM)	K_{D2}[b] (μM)	k_1 ($\mu M^{-1} s^{-1}$)	k_{-1} (s^{-1})	k_2 (s^{-1})	k_{-2} (s^{-1})	K_D^{calc} [c] (μM)
RRE-72AP + Rev	0.020 ± 0.007		140 ± 15	8 ± 4	11 ± 1	3 ± 1	0.016 ± 0.005
RRE + Neo	0.25 ± 0.05	1.9 ± 0.6					

[a] Measurements were made in the high ionic strength standard buffer at 10 °C. The thermodynamic parameters represent average values from different experiments, and the errors are standard uncertainties. The kinetic constants correspond to the two-step binding mechanism in eqs 3 and 4. [b] This dissociation constant corresponds to the competitive binding site for Rev and is the average value from the experiments in Figure 5B,C; additional weaker neomycin binding sites with K_D values in the high micromolar to millimolar range were also detected (see text). [c] This dissociation constant for Rev binding to RRE-72AP was calculated from the kinetic constants (i.e., $K_D^{calc} = k_{-1}k_{-2}/k_1k_2$).

the complex (Figure 1B). By fitting the data shown in Figure 2 to eq 1, a $K_D = 13 \pm 2$ nM for Rev peptide binding at 10 °C was calculated. In additional measurements in which the RRE-72AP concentration was varied from 30 to 100 nM ($n = 3$), an average K_D value of 20 ± 7 nM for Rev binding was determined. This average value agrees well with the $K_D = 15 \pm 5$ nM that was previously measured at 15 °C by following fluorescence anisotropy changes of fluorescein-labeled Rev peptide upon binding to the native RRE sequence (*18*). Thus, these similar results, which were obtained using the same solution conditions and nearly identical RNA and peptide constructs, demonstrate that the 72AP probe does not significantly affect Rev affinity for RRE.

In contrast with the 72AP label, Rev titration of RRE-68AP produced no fluorescence change (Figure 2B), suggesting that the environment of the 68AP label does not change upon Rev binding. The alternative explanation that the 68AP label has a deleterious effect on Rev binding is excluded by the competition binding experiment in Figure 5C (see below), as well as electrophoretic mobility shift experiments which showed that the native RRE and the two 2-AP constructs were shifted in the same concentration range of Rev (data not shown).

Stopped-Flow Kinetic Analysis of Rev Peptide Binding. Stopped-flow kinetic experiments indicate that Rev binding to RRE-72AP occurs in two kinetic phases, which suggests a two-step binding mechanism (Figure 3A). The first faster kinetic phase is found to be linearly dependent on Rev concentration, while the second slower phase follows approximately a hyperbolic dependence on Rev concentration (Figure 3B). For this type of mechanism (eqs 3 and 4), the slope of the linear phase is equal to the observed on-rate (k_1[Rev] + k_{-1} + k_2 + k_{-2}), and the *y*-intercept is equal to the sum of $k_{-1} + k_2 + k_{-2}$ (*46*). For the hyperbolically dependent phase, the asymptotic rate is equal to the sum $k_2 + k_{-2}$, and the *y*-intercept provides a crude estimate of the off-rate. The four microscopic rate constants describing this mechanism were partially illuminated by curve fitting to eq 3, which allows direct determination of k_1 and k_{-1}, and the sums $k_2 + k_{-2}$ and $k_{-1} + k_2 + k_{-2}$.

To determine the remaining rate constants, k_2 and k_{-2}, a better estimate of the off-rate was made using a trapping experiment. In this experiment (Figure 3C), a complex between Rev and RRE-72AP was rapidly mixed with a large excess of neomycin, such that peptide dissociation was made irreversible. Thus, a single-exponential rate of peptide dissociation is observed with a rate constant $k_{off} = k_{-1}k_{-2}/(k_{-1} + k_2 + k_{-2}) = 1.7 \pm 0.1\ s^{-1}$. This measurement, in conjunction with the known sum $k_{-1} + k_2 + k_{-2}$, allowed calculation of the product $k_{-1}k_{-2}$, which along with the known sum $k_2 + k_{-2}$ allowed calculation of the individual rate constants k_2 and k_{-2}. The calculated rate constants for this two-step mechanism are reported in Table 1. The overall $K_D = 16 \pm 5$ nM for Rev binding that is calculated from the microscopic rate constants agrees well with the $K_D = 20$ nM determined from the equilibrium measurements. Thus, the two-step mechanism is consistent with the thermodynamic measurements on this system.

Aminoglycosides Bind to Multiple Sites on RRE. To test whether the same fluorescent probes might be used to directly detect aminoglycoside binding to RRE, titration experiments with RRE-68AP and RRE-72AP were performed (Figure 4). As shown in Figure 4A, titration of RRE-68AP with neomycin results in a fluorescence change that occurs in two phases. In the first phase, a 1.3-fold increase in the fluorescence signal occurs, which plateaus at a neomycin

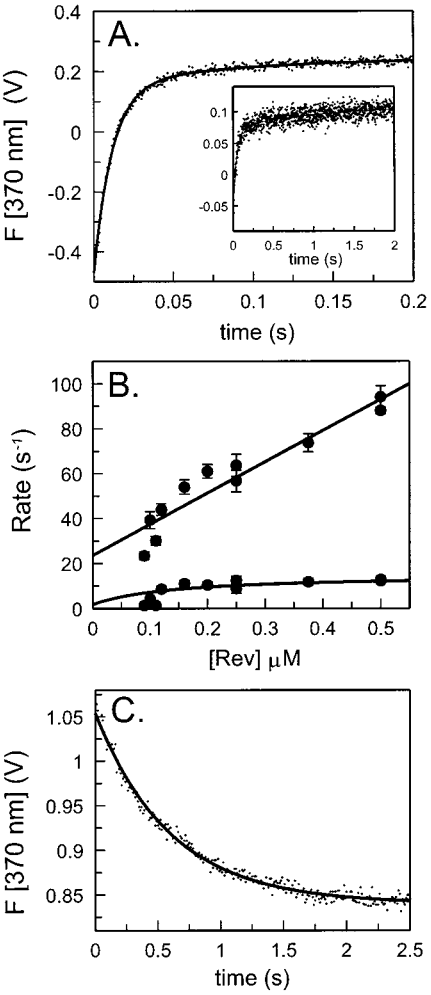

FIGURE 3: Stopped-flow kinetic measurements of Rev binding to RRE-72AP RNA. (A) Fluorescence change upon rapid mixing of RRE-72AP with Rev (final concentrations of 100 and 500 nM, respectively). The trace was fit to a double exponential equation ($k_1 = 87$ s^{-1}, $k_2 = 11$ s^{-1}). The inset shows data obtained at 20 nM RRE-72AP and 90 nM Rev concentration ($k_1 = 24$ s^{-1}, $k_2 = 0.94$ s^{-1}). (B) Concentration dependence of the two kinetic phases of Rev binding. (C) Determination of the Rev off-rate from RRE-72AP using neomycin as a irreversible trap for the free RNA. A complex consisting of 100 nM each RRE-72AP and Rev was rapidly mixed with a solution of 100 μM neomycin. A k_{off} of 1.7 s^{-1} for Rev was determined from this experiment.

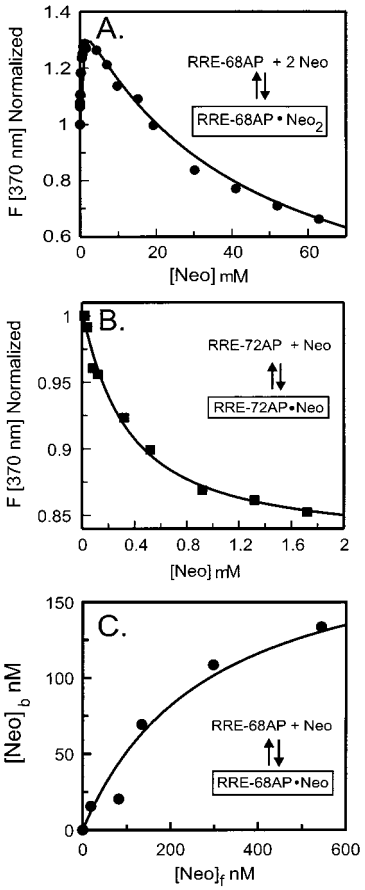

FIGURE 4: Fluorescence changes accompanying titration of 2-AP-labeled RRE with neomycin. (A) Titration of 100 nM RRE-68AP with increasing concentrations of neomycin. The relative fluorescence increase at 370 nm as a function of total neomycin concentration is plotted. The best-fit curve to a two-site binding model is shown ($K_{D1} = 0.23 \pm 0.03$ μM, $K_{D2} = 41 \pm 6$ μM). (B) Relative fluorescence changes at 370 nm for the RRE-72AP construct as a function of total neomycin concentration. The data are fitted to eq 1 with a $K_D = 0.29 \pm 0.07$ μM. (C) Binding of neomycin to RRE-68AP as determined by equilibrium ultrafiltration measurements. The curve is a fit to eq 2 ($K_D = 0.29 \pm 0.04$ μM). The species that is directly detected in each experiment is marked with a box in each panel.

concentration of approximately 1 μM. Continued titration with neomycin over the range 10−100 μM results in an overall 50% decrease in the original RRE-68AP fluorescence signal. When these data were fit by computer simulation to the simplest model involving neomycin binding to two noninteracting sites on RRE-68AP (see curve in Figure 4A), K_D values of 230 ± 30 nM and 41 ± 6 μM were calculated. As shown below, a moderate affinity binding site for neomycin is revealed in competitive binding experiments with the Rev peptide ($K_D = 1.9$ μM), but this site is not detected in these direct neomycin binding experiments using either the 72AP or the 68AP probes. For simplicity, we have not included this moderate affinity site in the analysis of the data in Figure 4 because inclusion of this "transparent" binding event has little effect on the apparent K_D values for the observed tight and weak sites (not shown).

In contrast with RRE-68AP, the 72AP construct shows a monotonic 15% decrease in fluorescence intensity over the neomycin concentration range 0−2 μM (Figure 4B). Using eq 1, a K_D value of 290 ± 70 nM for neomycin binding to RRE-72AP was determined, which is nearly identical to the K_D determined for the higher affinity site using the 68AP label. For the RRE-72AP construct, a further 10% linear decrease in fluorescence was observed as the neomycin concentration was increased from 10 to 200 μM. This decrease is most likely attributable to binding to very weak sites with binding constants in the low millimolar range, and was not analyzed further. These results, using two different reporter groups, suggest that neomycin binds to a tight site on RRE RNA ($K_D \sim 250$ nM), as well as a weaker site (or sites) with K_D values in the high micromolar to millimolar range.

Since the 2-AP fluorescence assay for neomycin binding only detects *bound* ligand, we sought to confirm the presence of the tight neomycin binding site by an equilibrium ultrafiltration method in which *free* neomycin is directly measured (Figure 4C). In this centrifugal filtration procedure (*17*), a membrane retains neomycin that is bound to RRE-68AP, while free neomycin passes through the membrane.

The neomycin in the filtrate and retentate may then be quantified by post-labeling with ^{32}P using [γ-^{32}P]ATP and the enzyme neomycin phosphotransferase II. The dissociation constant for neomycin binding to its tight site determined using this procedure is indistinguishable from that found using the fluorescence assay ($K_D = 290 \pm 38$ nM), which unambiguously establishes the presence of this tight site for neomycin binding to RRE. Since the ultrafiltration assay is not well suited for determining neomycin binding to weaker sites on RRE, only the tighter site was investigated using this procedure.

Occupation of the Tight Neomycin Binding Site Is Not Inhibitory to Rev Peptide Binding. To determine which neomycin binding site was inhibitory to Rev binding, three different competition binding experiments were performed (Figure 5). In the first experiment (Figure 5A), a RRE-72AP−neomycin complex was titrated with increasing concentrations of Rev. In this experiment, the neomycin concentration was fixed at 990 nM so that the tight neomycin binding site was 80% occupied, and the weakest site detected in the direct neomycin binding experiments of Figure 4A was less than 1% occupied ($K_D = 41$ μM). Thus, if occupation of the tighter site affects Rev binding, a higher apparent K_D value for Rev binding should be measured under these conditions. When Rev binds to the RRE-72AP−neomycin complex, a 2.2-fold fluorescence increase is observed which is indistinguishable from that seen in the absence of neomycin (compare Figures 5A and 2B). Fitting the data of Figure 5A to a model in which neomycin does not perturb the interaction of Rev with its site (eq 1) yielded an apparent K_D of 28 ± 11 nM for Rev (see solid curve in Figure 5A), which is only slightly greater than the value measured in the absence of neomycin (see curve with short dashes in Figure 5A; $K_D = 20$ nM). In contrast, if neomycin binding to its tight site were directly competitive with Rev binding, the expected Rev binding curve would deviate considerably from the observed data (see theoretical curve with long dashed lines in Figure 5A). Thus, these results are consistent with the proposal that occupation of the tight neomycin binding site is not inhibitory to Rev binding. As confirmed in the following experiments, the slightly weaker apparent K_D value for Rev under these conditions suggests that partial occupation of another weaker neomycin binding site is inhibitory to Rev binding.

In a second complementary experiment, we asked if Rev binding to its site on RRE affected the affinity of neomycin for its tighter site. Thus, a competitive binding experiment was performed in which a RRE-72AP−Rev complex was titrated with increasing concentrations of neomycin (Figure 5B). In this experiment, two distinct fluorescent phases were observed. In the first phase, a 15% decrease in fluorescence was observed as the neomycin concentration was increased from 0 to 2 μM. The amplitude of this initial fluorescence drop is similar to that shown in Figure 4B when free RRE-72AP is titrated with neomycin, again suggesting that the tight neomycin site is occupied independently from Rev. As the neomycin concentration was increased further, the fluorescence continued to drop to a plateau level about 3.2-fold less than that of the initial RRE-72AP−Rev complex. This is close to the expected change if the fluorescence decrease due to neomycin binding to its tight site and the decrease due to the displacement of Rev from its site are additive.[3] From the data in Figure 5B, a K_D of 2.0 ± 0.6 μM for neomycin binding to the competitive site was calculated employing the simplest model in which neomycin binds to a tight site ($K_D = 250$ nM), and then a second neomycin binds competitively with Rev for a second weaker site. In this fitting procedure, the K_D values for the neomycin

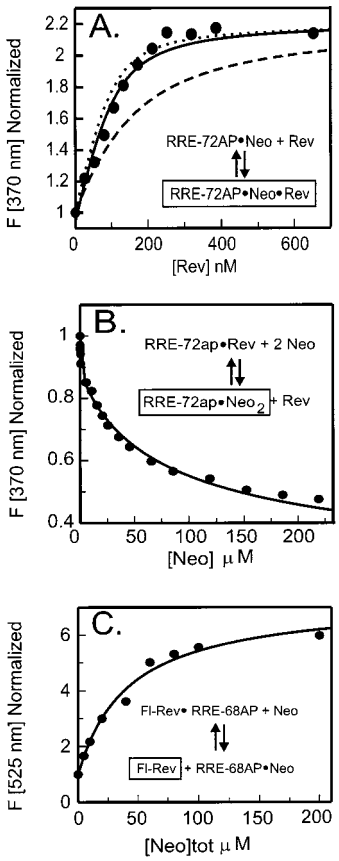

FIGURE 5: Dual binding of neomycin and Rev to RRE-72AP. (A) Titration of a complex between RRE-72AP ($[RRE]_{tot} = 100$ nM) and neomycin ($[Neo]_{tot} = 990$ nM) with Rev peptide. The solid curve is a best fit to eq 1, which yields a K_D of 29 ± 10 nM for Rev binding when the tight neomycin site is 81% occupied. The short and long dashed curves are the calculated binding isotherms if Rev peptide binding is independent or competitive with occupation of the tight neomycin binding site, respectively. The similarity of the solid and short dashed-line curves indicates that neomycin binding to its tight site does not affect Rev binding to its site. (B) Titration of a complex between RRE-72AP ($[RRE]_{tot} = 200$ nM) and Rev ($[Rev]_{tot} = 500$ nM) with neomycin. The curve was calculated using the program *Dynafit* (*40*) using a model in which neomycin binds independently to a tight site ($K_D = 0.23$ μM), and then competitively with Rev for a second site ($K_D = 1.9 \pm 0.6$ μM). (C) Displacement of Fl-Rev (450 nM) from RRE-68AP (500 nM) by neomycin as determined in an equilibrium ultrafiltration experiment. The curve was calculated using the program *Dynafit* (*40*) employing a model in which neomycin binds independently to a tight site ($K_D = 0.23$ μM), and then competitively with Rev for a second site ($K_D = 1.8 \pm 0.8$ μM). The species that is directly detected in each experiment is marked with a box in each panel. In the analysis of panels B and C, neomycin binding to weaker sites ($K_D > 40$ μM) was not included because such events are 20-fold weaker than neomycin binding to the inhibitory site.

[3] The observed fluorescence decrease is attributed solely to the release of Rev, and cannot be attributed to direct fluorescence quenching by neomycin binding to the competitive site, because control experiments showed a linear decrease of only 10% when the neomycin concentration was varied in the range 10−200 μM, and this effect is corrected for in the experiment shown in Figure 5B.

tight site and the Rev binding site were held fixed at their average values of 250 and 20 nM, respectively, while the K_D for the second competitive neomycin site and the fluorescence amplitudes were allowed to vary.

Finally, to establish that occupation of the tighter neomycin binding site is not inhibitory to Rev binding and to confirm the presence of a neomycin−Rev−RRE ternary complex, we performed an equilibrium ultrafiltration experiment with amino-terminal fluorescein-labeled Rev (Fl-Rev). This Rev peptide construct has been previously shown to bind to RRE with the same affinity and specificity as the native Rev peptide (*18*), and allows sensitive fluorescence measurements of the peptide to be performed. In this experiment (Figure 5C), a complex between Fl-Rev and RRE-68AP was competed with increasing concentrations of neomycin. Since free Fl-Rev passes through the membrane filter, while the larger Fl-Rev−RRE complex is retained, this approach allows a direct determination of *free* Fl-Rev as a function of total neomycin concentration. Curve fitting the data as described above using the simplest model in which neomycin binds to a tight site (K_D = 250 nM), and then Fl-Rev and neomycin compete for a second binding site, yields a K_D of 1.8 ± 0.6 μM for neomycin binding to the inhibitory site. This K_D is in excellent agreement with the value determined in Figure 5B using 2-AP fluorescence changes, and establishes that the tight and inhibitory neomycin binding sites are *distinct*. We point out here that the inhibitory site detected in these competition assays is *not* the same weak site that is detected in the direct neomycin binding assay (Figure 4A, K_D = 41 μM). We therefore conclude that neomycin binding to the inhibitory site is silent with respect to the 68AP and 72AP probes, and is only detected in competition experiments with Rev.

NMR Evidence for an RRE−Neomycin Complex and an RRE−Rev−Neomycin Ternary Complex. The formation of the binary neomycin−RRE complex was followed by monitoring changes in the imino proton spectrum of RRE upon titration with neomycin (Figure 6A). The imino proton chemical shift assignments for free RRE were made by inspection of 2D NOESY spectra (data not shown), and were found to match those determined previously (*11*). Upon addition of neomycin to free RRE, obvious perturbations are observed for a subset of imino proton resonances. By inspection of the 2D NOESY spectrum of the RRE−neomycin complex in Figure 6B, the imino protons that shift (G42, G46, G67, and G77), broaden (U45 and U43), and sharpen (G46) upon titration can be unambiguously assigned (see figure legend for details). By inspection of the RRE secondary structure in Figure 1A, it may be concluded that all of the perturbed residues, with the exception of G67, are located in the *lower stem* of RRE. The chemical shift perturbation of G67, which forms a base pair with C49 at the upper stem−bulge junction, is most simply accounted for by an indirect allosteric effect of neomycin binding to the lower stem. This NMR result is in accord with the observation that neomycin binding perturbs the fluorescence of the adjacent bulge residue, 68AP (Figure 4A).

To monitor the course of the neomycin titration of RRE, we followed the chemical shift changes for residue G77 because these changes are clearly followed in the 1D spectra (Figure 6A). Before addition of neomycin, the imino proton of G77 shows a single resonance. Upon addition of 0.65 equiv of neomycin, the single resonance for G77 is split into two resonances with nearly equal intensity. This behavior indicates that free neomycin and bound neomycin are in slow exchange on the chemical shift time scale. Consistent with this interpretation, when a slight molar excess of neomycin is added, a single resonance is once again observed for G77 that has the same chemical shift of the second resonance that appeared at the substoichiometric neomycin concentration. We point out that under the conditions of the NMR titration experiments only the tightest neomycin site is significantly occupied, because affinity for this site is ≥8

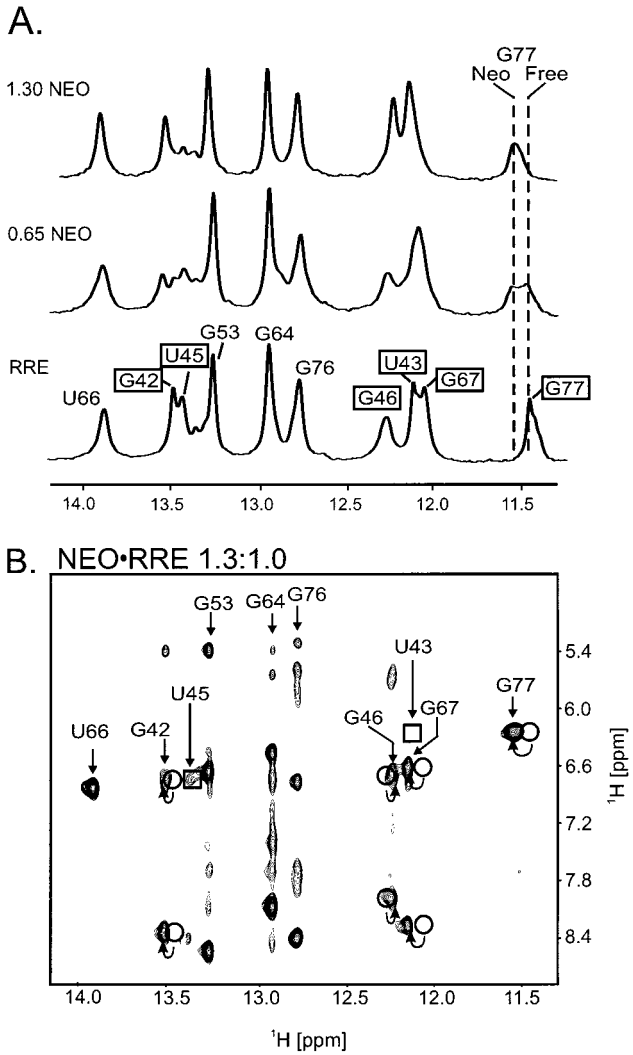

FIGURE 6: Titration of RRE with neomycin resulting in the formation of a specific binary neomycin−RNA complex. (A) 1D proton spectra of the imino region of free RRE (lower spectrum), and RRE in the presence of 0.65 and 1.3 molar equiv of neomycin. Assignments for free RRE are shown (*11*). Imino protons that show chemical shift perturbations upon addition of neomycin are boxed. The free and bound imino resonances of G77 are indicated with dashed lines. (B) Imino−aromatic proton region of NOESY spectra of the neomycin−RNA binary complex at 15 °C in 90% H_2O/10% D_2O showing the chemical shift changes observed in this region of the spectra upon binding of neomycin. The resonances that change in the 1D spectra may be assigned in this 2D spectrum. Cross-peaks are labeled by imino proton assignments. Open circles indicate the position of imino to aromatic/amino correlated cross-peaks before addition of neomycin, and the curved arrows indicate the direction of the chemical shift change. The positions of cross-peaks in the free RRE that are observed to broaden upon neomycin binding are boxed.

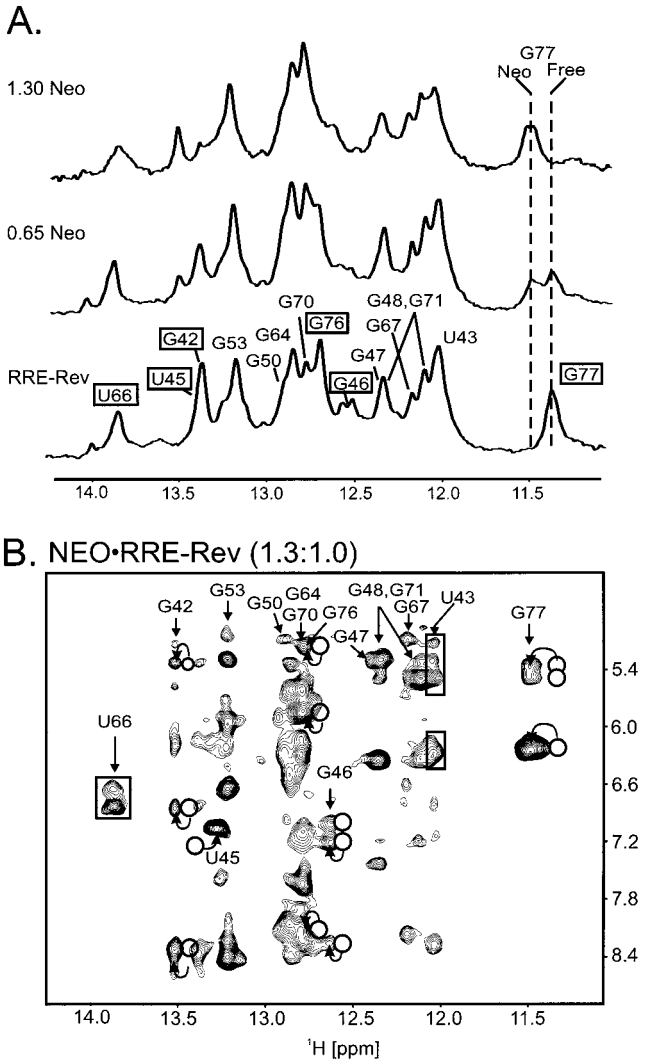

FIGURE 7: Titration of the RRE−Rev complex with neomycin resulting in the formation of a specific ternary neomycin−RNA−peptide complex. (A) 1D proton spectra of the imino region of the RRE−Rev complex (lower spectrum), and the complex in the presence of 0.65 and 1.3 molar equiv of neomycin. Assignments for the RRE−Rev complex are shown (*11*). Imino protons that show chemical shift perturbations upon addition of neomycin are boxed. The free and bound imino resonances of G77 are indicated with dashed lines. (B) Imino−aromatic proton region of NOESY spectra of the neomycin−RRE−Rev ternary complex at 15 °C in 90% H_2O/10% D_2O showing the chemical shift changes observed in this region of the spectra upon binding of neomycin. The resonances that change in the 1D spectra may be assigned in this 2D spectrum. Cross-peaks are labeled by imino proton assignments. Open circles indicate the position of imino to aromatic/amino correlated cross-peaks before addition of neomycin, and the curved arrows indicate the direction of the chemical shift change. The positions of cross-peaks in the RRE−Rev complex that are observed to broaden upon neomycin binding are boxed.

times greater than the second site detected in fluorescence titration experiments using identical conditions (data not shown).

To ascertain whether we could detect a ternary complex between neomycin, RRE, and the Rev peptide using NMR methods, we titrated the binary RRE−Rev complex with neomycin (Figure 7A). The imino proton chemical shift assignments for the RRE−Rev complex were made by inspection of 2D NOESY spectra (data not shown), and were found to match those previously determined (*11*). The titration of the RRE−Rev complex with neomycin (Figure 7A,B) results in shift changes or broadenings for the same residues in the lower stem that were affected in the neomycin titration of the free RNA (i.e., G42, G46, U43, and G77), suggesting that neomycin binds in an indistinguishable fashion to the lower stem in both free RRE and the RRE−Rev complex. As observed for the neomycin titration of RRE, neomycin titration of the RRE−Rev complex again indicates that free neomycin and bound neomycin are in slow exchange on the chemical shift time scale (Figure 7A) as judged by the chemical shift changes for residue G77. Moreover, addition of 1.3 equiv of neomycin to the RRE−Rev complex does not significantly perturb the imino proton chemical shifts for the bulge base pairs that are stabilized upon Rev binding, providing strong evidence that the peptide remains bound and unchanged in its interaction with RRE in the presence of 1 equiv of neomycin.

In addition to the common residues that were perturbed in the free RNA, neomycin titration of the RRE−Rev complex also resulted in chemical shift perturbations for the imino proton resonances of G76 and U45, located in the lower stem, and a significant broadening of the imino proton resonance of U66, located in the upper stem. Since the noninhibitory tight binding site for neomycin is suggested to be in the lower stem region, the changes observed for U66 must be explained by a long-range allosteric effect of neomycin binding on the RNA conformation or dynamics, as was observed for residues G67 and 68AP in free RRE (see above). In summary, these NMR spectra provide strong support for a single neomycin binding site that is not competitive with Rev, and suggest that this same neomycin binding site, located in the lower stem region of RRE by chemical shift perturbation data, exists in both the free RNA and the RNA−peptide complex.

DISCUSSION

Mechanism of Specific Rev Peptide Binding to RRE. The intact HIV-1 Rev protein is a 16 kDa RNA-binding protein that cooperatively binds the 244-nucleotide full-length RRE with a stoichiometry of 4 Rev monomers per RRE (*47*). The mechanism of RRE binding by the Rev protein has been studied using surface plasmon resonance methods, and is thought to occur by the initial binding of a Rev monomer to the high-affinity stem−loop region of RRE, followed by oligomerization of Rev mediated by protein−protein contacts (*47*). The short α-helical peptide corresponding to the arginine-rich RNA binding domain of Rev binds specifically to the stem−loop IIB of RRE, providing a good model system to study the initial process of monomer recognition of the stem−loop, without complications from protein oligomerization (*8*−*14*). In addition, a high-resolution NMR structure of the Rev peptide bound to RRE has been solved (*12*), which provides a structural framework from which to interpret the binding process.

We have shown here that Rev peptide binding to RRE occurs in two steps: an initial encounter followed by isomerization of the RNA (Figure 3, Table 1). The initial encounter step is very rapid, occurring with a second-order rate constant of $\sim 10^8$ M^{-1} s^{-1} that is in the range of values expected for diffusion-controlled encounter of molecules of this size. The large value of this rate constant for formation

of the encounter complex suggests that both the free peptide and free RNA are in the correct conformation to bind, and that any reorganization of the RNA or peptide that occurs during formation of this initial encounter complex is extremely rapid. The low K_D value for the Rev peptide is largely the result of this diffusion-controlled on-rate, as the off-rate is fairly fast (1.7 s^{-1}, Table 1).

The significant increase in fluorescence that occurs upon forming the initial complex with RRE-72AP suggests that the 72AP base becomes more exposed (less stacked) upon peptide binding. This result is consistent with the NMR structure of the Rev peptide−RRE complex, which shows that the bulge residue U72 is flipped-out of the A-helix, and that a critical purine−purine base pair is formed between G71 and G48 (Figure 1A). This new base pair acts to widen the RNA major groove by 5 Å, allowing deep penetration of the peptide and the formation of key hydrogen-bonding or electrostatic interactions with the arginine-rich motif of Rev (*12*). The second slower kinetic transient, which has a smaller amplitude, may represent a final docking step in which the RNA and peptide isomerize into the final conformation. This docking step contributes only 3-fold to the total free energy of binding (i.e., $k_2/k_{-2} = K_2 = 3$, Table 1). Thus, the bulk of the interaction energy between the peptide and RNA has been realized in the initial encounter complex.

It is of interest to note that the 68AP label, which is at the junction of the bulge and upper stem, shows no fluorescence change upon Rev peptide binding. Residue A68 is proposed to be stacked below residue G67 of the upper stem of free RRE on the basis of G67H8−A68H8 and G67H1′−A68H8 NOEs (*11*), but is completely flipped-out in the NMR structure of the complex (*12*). Thus, this type of environment change would be expected to result in a significant increase in 2-AP fluorescence. The absence of a detectable increase in 68AP fluorescence and its relatively high initial fluorescence, as observed in Figure 2, suggest that 68AP is also highly exposed in the free RNA, and that a smaller change in its environment occurs upon Rev peptide binding. These apparent differences may reflect dynamic behavior at the junction between the bulge and upper stem, or weak stacking between A68 and G67 in the free RNA that does not lead to strong quenching of the 2-AP fluorescence.

Where Does Neomycin Bind on RRE? Although aminoglycosides have a general affinity for RNA, and operate as potent antibacterial agents by binding to specific regions of rRNA in prokaryotes (*48*), little is known about the structural features in RNA that are essential for specific aminoglycoside binding. It has been suggested on the basis of chemical modification and protection experiments, as well as mutational studies (*15, 17*), that neomycin B binding to RRE is favored in nonhelical regions, with a distinct preference for the internal purine-rich bulge. In fact, the general proposal has been made that aminoglycosides bind preferentially to regions where structural perturbations have widened the RNA major groove (*18, 49*−*54*). However, these conclusions are inconsistent with SPR measurements of neomycin binding to RRE, and a variant of RRE in which the bulge region was replaced with canonical base pairs (*16*), where no difference was observed in the binding affinity of neomycin in the absence and presence of the bulge. In addition, there appears to be at least one exception to the general rule that aminoglycosides bind preferentially to the RNA major groove. In studies of neomycin binding to the TAR element of HIV-1 RNA, it was found that inosine substitutions in the lower stem decreased neomycin binding by 100-fold, suggesting that the aminoglycoside is bound in the minor groove of the lower stem in TAR (*55*).

The present results indicate that neomycin B binds to RRE with a stoichiometry of 3 neomycins for each RNA in the concentration range investigated. The tightest site ($K_D = 250$ nM) is not inhibitory to Rev binding. The intermediate affinity site inhibits Rev binding in a competitive fashion ($K_D = 1.9$ μM), and the third very weak site(s) is (are) attributed to nonspecific binding ($K_D = 41$ μM). The observation of a three-site stoichiometry for neomycin binding to RRE, with a specific high-affinity neomycin binding site that is noninhibitory to Rev binding, is in contrast with previous published neomycin binding data determined using competitive binding assays (*18, 19*). However, the three-site stoichiometry is very similar to that observed by Hendrix et al., who used SPR methods to study these complexes (*16*). Since both the present 2-AP fluorescence study and previous SPR study monitor neomycin binding events directly, it clearly appears that these methods are able to detect binding events that escaped detection in competitive binding assays.

NMR chemical shift perturbations suggest that the high-affinity site for neomycin is located on the lower stem of free RRE and the RRE−Rev complex. One possible model is that the aminoglycoside binds in the broad and shallow minor groove of the lower stem, in a fashion similar to that observed for neomycin binding to TAR. Such a model could explain why neomycin binding to the tight site has no significant effect on Rev peptide binding to the major groove of RRE, which is widened by the formation of purine−purine base pairs in the bulge. We could not obtain evidence to confirm or dispel this model using 2D ^{1}H NMR methods, because unambiguous intermolecular NOEs between neomycin and RRE were obscured by severe overlap of proton resonances. Therefore, further characterization of neomycin binding to RRE and RRE−Rev will require isotope labeling of the RNA and peptide (*12, 56, 57*).

Long-Range Effects of Neomycin Binding. The above conclusion that the tight noninhibitory neomycin binding site is located on the lower stem is surprising because the 68AP and 72AP fluorescent reporter groups used to detect neomycin binding in this study are located in the bulge region of free RRE (Figure 8A). These results suggest that neomycin binding to the lower stem alters the environment of the 72AP and 68AP bases through an allosteric mechanism. Such allosteric effects need not cause a large change in the average conformation of the RNA because in the steady-state fluorescence experiments used here, the observed spectra are the weighted average of the populations and lifetimes of all the states that are present. Therefore, the neomycin-induced changes in the 68AP and 72AP fluorescence intensities could simply result from a small change in the population of a state with a significantly different fluorescence lifetime (*27*). The effects of neomycin binding on the chemical shift of the upper stem residue G67 in free RRE, and the imino proton line width of the adjacent residue U66 in the RRE−Rev complex, also suggest long-range allosteric effects of neomycin binding to its tight site. The subtle changes in the

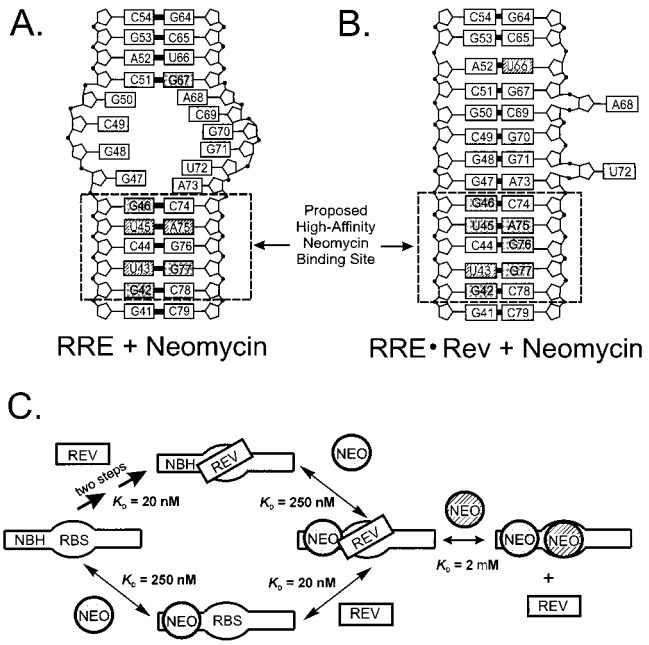

FIGURE 8: Thermodynamic, kinetic, and structural model for neomycin and Rev peptide binding to RRE. (A) Sequence of RRE with nucleotides shaded to indicate chemical shift perturbations of proton resonances belonging to this base upon neomycin binding or hatched to indicate broadening of proton resonances belonging to this base upon neomycin binding. The proposed high-affinity neomycin binding region of neomycin on RRE is boxed. (B) The kinetic/thermodynamic model for neomycin binding to RRE and RRE−Rev. Taken together, the fluorescence binding assays and NMR results suggest that neomycin binds to a tight site (shaded circle) on the lower stem (NBH, high-affinity neomycin binding site), and to a weaker site (hatched circle) on the bulge that overlaps with the Rev binding site (RBS). Kinetic studies indicate that Rev binds by a two-step mechanism involving isomerization of RRE. Binding of neomycin to its tight site has no discernible effect on Rev binding to its site. Note that binding of neomycin to the weak noncompetitive site is not considered in our model.

environment of these residues upon neomycin binding in the lower stem could reflect the highly dynamic and flexible nature of the bulge region, which allows upper stem residues that border the bulge to "feel" binding events in the lower stem. We note that an allosteric mechanism involving a transient ternary complex has been invoked in the Tat−Tar system to explain how binding of neomycin in the lower stem prevents Tat peptide binding to the bulge region of Tar RNA (*55*). The present case differs, however, because the allosteric effects of neomycin binding to the stem have no discernible effect on peptide binding to the bulge. We speculate that such long-range effects of aminoglycoside binding to RNA may be more common than previously thought, and may be a general feature of their mode of action.

The tight neomycin site detected here using 2-AP fluorescence would have eluded detection in previous chemical modification studies that used single-strand-specific reagents (*15*, *17*). However, this lower stem site probably represents the tight neomycin binding site that was detected in several previous binding studies. In this previous work from several groups, similar low K_D values for neomycin binding of 82 nM (*17*), 150 nM (*19*), and 210 nM (*16*) were reported. These K_D values were always significantly less than the measured K_i values of 1−2 μM for neomycin inhibition of Rev binding, suggesting the existence of multiple neomycin binding sites on RRE (*15*, *18*). The present results with respect to neomycin inhibition of Rev binding are consistent with these previous studies, and suggest that the inhibitory and noninhibitory sites are located in the bulge and lower stem regions, respectively (Figure 8). These results suggest a strategy for drug development in which the tight site may be converted into an inhibitory site through appropriate chemical modifications of the aminoglycoside (*20*−*26*).

ACKNOWLEDGMENT

We thank Dr. F. Song for synthesis of the 2-AP-labeled RRE constructs and Dr. T. E. Shrader (Albert Einstein College of Medicine) for generously providing us with plasmid (pT7-911Q) constructed in his laboratory.

REFERENCES

1. Daly, T. J., Cook, K. S., Gray, G. S., Maione, T. E., and Rusche, J. R. (1989) *Nature 342*, 816−819.
2. Felber, B. K., Hadzopoulou-cladaras, M., Cladaras, C., Copeland, T., and Pavlakis, G. N. (1989) *Proc. Natl. Acad. Sci. U.S.A. 86*, 1495−1499.
3. Malim, M. H., Hauber, J., Fenrick, R., and Cullen, B. R. (1988) *Nature 335*, 181−183.
4. Zapp, M. L., and Green, M. R. (1989) *Nature 342*, 714−716.
5. Cochrane, A. W., Chen, C. H., and Rosen, C. A. (1990) *Proc. Natl. Acad. Sci. U.S.A. 87*, 1198−1202.
6. Kjems, J., Frankel, A. D., and Sharp, P. A. (1991) *Cell 67*, 169−178.
7. Cook, K. S., Fisk, G. J., Hauber, J., Usman, N., Daly, T. J., and Rusche, J. R. (1991) *Nucleic Acids Res. 19*, 1577−1583.
8. Kjems, J., Calnan, B. J., Frankel, A. D., and Sharp, P. A. (1992) *EMBO J. 11*, 1119−1129.
9. Tan, R. Y., Chen, L., Buettner, J. A., Hudson, D., and Frankel, A. D. (1993) *Cell 73*, 1031−1040.
10. Tan, R. Y., and Frankel, A. D. (1994) *Biochemistry 33*, 14579−14585.
11. Battiste, J. L., Tan, R. Y., Frankel, A. D., and Williamson, J. R. (1994) *Biochemistry 33*, 2741−2747.
12. Battiste, J. L., Mao, H. Y., Rao, N. S., Tan, R. Y., Muhandiram, D. R., Kay, L. E., Frankel, A. D., and Williamson, J. R. (1996) *Science 273*, 1547−1551.
13. Peterson, R. D., Bartel, D. P., Szostak, J. W., Horvath, S. J., and Feigon, J. (1994) *Biochemistry 33*, 5357−5366.
14. Peterson, R. D., and Feigon, J. (1996) *J. Mol. Biol. 264*, 863−877.
15. Zapp, M. L., Stern, S., and Green, M. R. (1993) *Cell 74*, 969−978.
16. Hendrix, M., Priestley, E. S., Joyce, G. F., and Wong, C. H. (1997) *J. Am. Chem. Soc. 119*, 3641−3648.
17. Werstuck, G., Zapp, M. L., and Green, M. R. (1996) *Chem. Biol. 3*, 129−137.
18. Wang, Y., Hamasaki, K., and Rando, R. R. (1997) *Biochemistry 36*, 768−779.
19. Cho, J. H., and Rando, R. R. (1999) *Biochemistry 38*, 8548−8554.
20. Greenberg, W. A., Priestley, E. S., Sears, P. S., Alper, P. B., Rosenbohm, C., Hendrix, M., Hung, S. C., and Wong, C. H. (1999) *J. Am. Chem. Soc. 121*, 6527−6541.
21. Michael, K., Wang, H., and Tor, Y. (1999) *Bioorg. Med. Chem. 7*, 1361−1371.
22. Tok, J. B. H., and Rando, R. R. (1998) *J. Am. Chem. Soc. 120*, 8279−8280.
23. Tor, Y. (1997) *Abstr. Papers Am. Chem. Soc. 213*, 70-CARB.
24. Tok, J. B. H., Cho, J. H., and Rando, R. R. (1999) *Tetrahedron 55*, 5741−5758.
25. Wang, H., and Tor, Y. (1998) *Angew. Chem., Int. Ed. Engl. 37*, 109−111.
26. Park, W. K. C., Auer, M., Jaksche, H., and Wong, C. H. (1996) *J. Am. Chem. Soc. 118*, 10150−10155.

27. Stivers, J. T. (1998) *Nucleic Acids Res. 26*, 3837−3844.
28. Holz, B., Klimasauskas, S., Serva, S., and Weinhold, E. (1998) *Nucleic Acids Res. 26*, 1076−1083.
29. Nordlund, T. M., Evans, K. O., and Xu, D. (1998) *Biophys. J. 74*, A21.
30. Frey, M. W., Sowers, L. C., Millar, D. P., and Benkovic, S. J. (1995) *Biochemistry 34*, 9185−9192.
31. Marquez, L. A., and RehaKrantz, L. J. (1996) *J. Biol. Chem. 271*, 28903−28911.
32. Stivers, J. T., Pankiewicz, K. W., and Watanabe, K. A. (1999) *Biochemistry 38*, 952−963.
33. Menger, M., Tuschl, T., Eckstein, F., and Porschke, D. (1996) *Biochemistry 35*, 14710−14716.
34. Millar, D. P. (1996) *Curr. Opin. Struct. Biol. 6*, 322−326.
35. Giver, L., Bartel, D. P., Zapp, M. L., Green, M. R., and Ellington, A. D. (1993) *Gene 137*, 19−24.
36. Giver, L., Bartel, D., Zapp, M., Pawul, A., Green, M., and Ellington, A. D. (1993) *Nucleic Acids Res. 21*, 5509−5516.
37. Milligan, J. F., and Uhlenbeck, O. C. (1989) *Methods Enzymol. 180*, 51.
38. Milligan, J. F., Groebe, D. R., Witherell, G. W., and Uhlenbeck, O. C. (1987) *Nucleic Acids Res. 15*, 8783−8798.
39. Beaucage, S. L., and Caruthers, M. H. (1981) *Tetrahedron Lett. 22*, 1859.
40. Kuzmic, P. (1996) *Anal. Biochem. 237*, 260−273.
41. Dang, Q., and Frieden, C. (1997) *Trends Biochem. Sci. 22*, 317−317.
42. Piotto, M., Saudek, V., and Sklenar, V. (1992) *J. Biomol. NMR 2*, 661−665.
43. Lippens, G., Dhalluin, C., and Wieruszeski, J. M. (1995) *J. Biomol. NMR 5*, 327−331.
44. Delaglio, F., Grzesiek, S., Vuister, G. W., Zhu, G., Pfeifer, J., and Bax, A. (1995) *J. Biomol. NMR 6*, 277−293.
45. Flannery, B. P., Teukolsky, S. A., and Vetterling, W. T. (1992) *Numerical Recipes in Fortran*, 2nd ed., Cambridge University Press, Cambridge, U.K.
46. Johnson, K. A. (1992) *Enzymes (3rd Ed.) 20.*
47. Van Ryk, D. I., and Venkatesan, S. (1999) *J. Biol. Chem. 274*, 17452−17463.
48. Gale, E., Cundliffe, E., Reynolds, P., Richmond, M., and Waring, M. (1981) *The Molecular Basis of Antibiotic Action*, Wiley, London.
49. Cho, J. Y., Hamasaki, K., and Rando, R. R. (1998) *Biochemistry 37*, 4985−4992.
50. Wang, Y., and Rando, R. R. (1995) *Chem. Biol. 2*, 281−290.
51. Recht, M. I., Fourmy, D., Blanchard, S. C., Dahlquist, K. D., and Puglisi, J. D. (1996) *J. Mol. Biol. 262*, 421−436.
52. Llano-Sotelo, B., and Chow, C. S. (1999) *Bioorg. Med. Chem. Lett. 9*, 213−216.
53. Leclerc, F., and Cedergren, R. (1998) *J. Med. Chem. 41*, 175−182.
54. Fourmy, D., Recht, M. I., and Puglisi, J. D. (1998) *J. Mol. Biol. 277*, 347−362.
55. Wang, S. H., Huber, P. W., Cui, M., Czarnik, A. W., and Mei, H. Y. (1998) *Biochemistry 37*, 5549−5557.
56. Batey, R. T., Inada, M., Kujawinski, E., Puglisi, J. D., and Williamson, J. R. (1992) *Nucleic Acids Res. 20*, 4515−4523.
57. Nikonowicz, E. P., Sirr, A., Legault, P., Jucker, F. M., Baer, L. M., and Pardi, A. (1992) *Nucleic Acids Res. 20*, 4507−4513.

BI992932P